Quad Rhombus Pinwheel Shaped Microstrip Patch Antenna

Mahesh Shankar Pandey[1], Dr. Virendra Singh Chaudhary[2]

[1]*PhD. Research Scholar,* [2]*Reseach Guide, Deptt. of Electronics and Communication Engineering*

RKDF University Gandhinagar Bhopal India

Abstract - Wireless communications antennas with high data rates must be compact, have a lot of bandwidth, and be omnidirectional. Monopole Antennas can easily meet all of the following requirements. Because the arms of a dipole or monopole have a current distribution nature, this has no effect on the antenna's radiation patterns; it only impacts the input impedance. The Quad Rhombus Pinwheel Shaped Patch Antenna (QRPPA) is proposed for WLAN and WiMAX applications in this study. The planned Monopole antenna features a Quad Rhombus Pinwheel tuning stub and a defective ground structure powered by a microstrip feed line. The size of the radiating patch, as well as the dimensions of the defective ground and its notch, were optimized to produce an acceptable tuning of resonating frequencies. Quad Rhombus Pinwheel Shaped Patch antenna with a defective ground plane that covers the frequency range of 2.134 to 3.886 GHz and has a minimum return loss of -18 dB at the resonance frequency of 3.334 GHz.

Keywords – Quad, MSPA, Rhombus, Notch, Defected Ground.

I. INTRODUCTION

Current wireless communications are the different commercial wireless standards used for its organization and allocated frequency band that radio equipment are used to transmit and receive the data [1]. They have nonstop to evolve from 1G to 5G, that could support higher capability digital systems with incorporated [2-3].

In high data speed wireless communications antenna must have a small in size, have good bandwidth and also have a omni-directional characteristics [4]. These all above requirements could be easily reached by Monopole Antennas. As the arms of dipole or monopole has the nature of current distribution and this does not change radiation patterns of the antenna only it effects the input impedance [8].

Wideband frequency response for wireless data speeds and bandwidths to the internet for laptops, PDAs, and other wireless devices that operate in close proximity to one another and has evolved several times responding to the sustained user demands for higher bit-rates. GSM900, GSM1400, GSM1900, ISM, WLAN, Bluetooth, LTE, Wi-Fi, WiMAX come under the wideband applications [9-14].

II. ANTENNA GEOMETRY AND DESIGN

The antenna construction of the designed antenna is shown in Figure 4.1. The proposed QRPPA is made on a FR-4 substrate with a thickness of 1.6 mm, a Loss Tangent of 0.02, and a dielectric constant of 4.3. A defective Quad Rhombus shaped radiator is fed by a 50 microstrip feed line as the overall antenna geometry. In order to match correct impedance, the defective ground structure (DGS) is included into the ground plane, along with the notch in the middle. The increased fractional bandwidth of 58.206 percent was attained over a frequency band of 2.134 GHz - 3.886 GHz by modifying the patch and notch defects in the ground plane. The proposed QRPPA has a physical size of 30mm x 45mm, with all parameters listed in Table 2. To increase impedance matching, the arms of a defective quad rhombus form and a notch have been included to minimise coupling between the margins of the patch and the ground plane ($|S_{11}|$ -10 dB). On CST Microwave Studio, QRPPA was simulated and the antenna structure was adjusted.

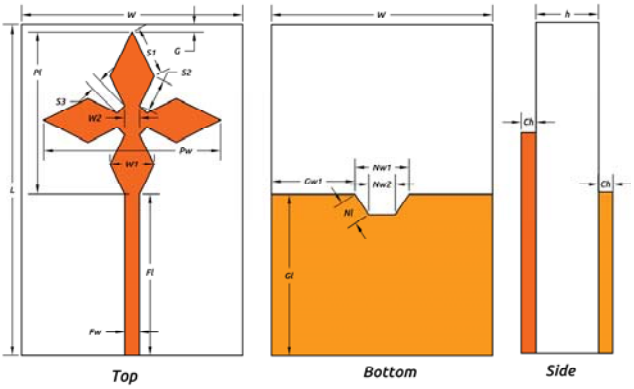

Figure 4.1 Antenna Structure

Table 4.1 Proposed Antenna's Dimensions

Parameter	***Dimension (mm)***	***Parameter***	***Dimension (mm)***
W	*30*	N_l	*3.37*
L	*45*	P_w	*24*
W_1	*6*	P_l	*22*

W_2	2	F_l	22
S_1	6.71	F_w	2
S_2	4.47	G_{w1}	11.33
S_3	1.41	G	1
N_{w1}	7.35	G_l	22
N_{w2}	3.60	h	1.6
C_h	0.035		

Table 4.2 Cut Off and Resonant Frequencies

Frequency	Notation	Value
Lower Cutoff	f_l	2.134 GHz
Higher Cutoff	f_h	3.886 GHz
First Resonance	f_{r1}	2.494 GHz
Second Resonance	f_{r2}	3.334 GHz

III. PARAMETRIC ANALYSIS

Parametric analysis by parametric sweep has been performed on several structural characteristics of the antenna in order to optimise its performance for bandwidth performance and suitable impedance matching. These additional parameters are adjusted within a given range in this section. One parameter is also varied to determine the exact influence on antenna performance.

3.1 Impact of Parameter Patch Width (P_w)

To demonstrate how patch width affects antenna performance, consider notch width P_w. patch width (P_w) is the radiator's width in the patch plane (see Figure 2(a)). During variation, the return loss characteristics were recorded and depicted in Figure 2(b). The breadth of the notch (P_w) varies from 23 to 24.5 mm.

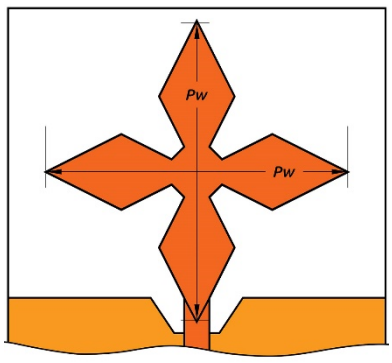

(a)

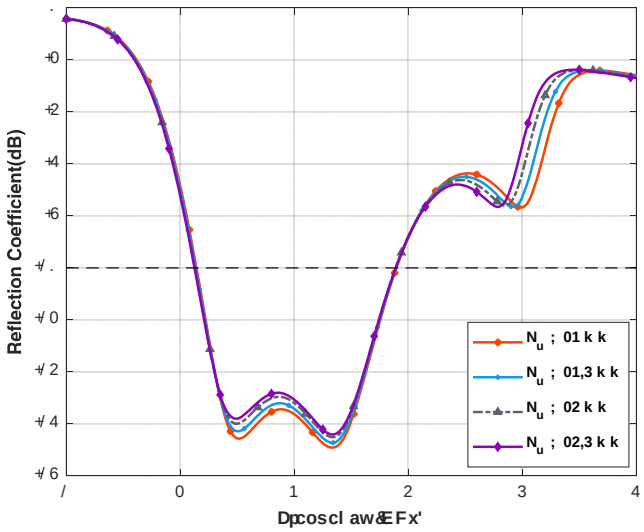

(b)

Figure 2 Parametric Analysis with Patch Width (Pw) (a) Antenna (b) Impact on Return Loss Characteristics

The return loss characteristics reveal that as the Notch width (P_w) grows, the antenna bandwidth rapidly expands. As a result, it can be inferred that a notch with a width of 24 mm provides the best bandwidth.

3.2 Impact of Parameter Pinwheel Leaf Width (W_1)

Pinwheel Leaf Width W_1 has been changed to see the effect of Pinwheel Leaf Width on antenna performance. This parameter is the patch plane's Pinwheel Leaf Width (see Figure 3(a)). During variation, the return loss characteristics were recorded and depicted in Figure 3(b). It ranges in size from 5 to 7 mm. The return loss characteristics reveal that as the antenna's bandwidth grows, it grows quickly and continues to grow. As a result, it can be stated that the antenna width of 7 mm is the ideal width for obtaining a broader bandwidth.

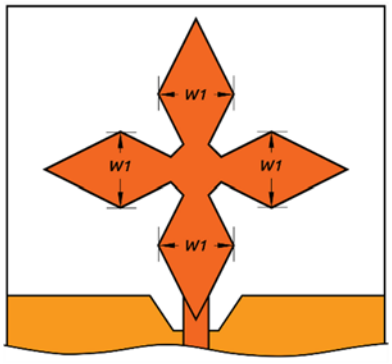

(a)

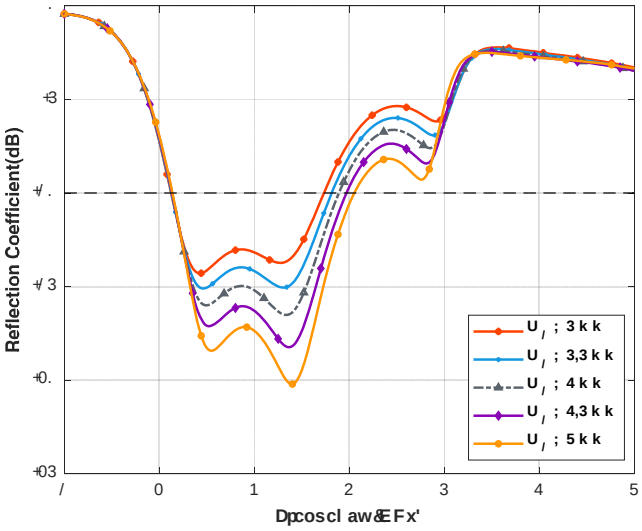

(b)

Figure 3 Parametric Analysis with Pinwheel Leaf Width (W_1) (a) Antenna (b) Impact on Return Loss Characteristics

3.3 Impact of Parameter Notch Upper Width (W_{n1}) Of Ground Notch

The upper notch width W_{n1} is changed to examine how it affects the antenna performance. Refer to Figure 4(a) for the top width of the notch formed on the ground plane opposite the patch and feedline joint. During variation, the return loss characteristics were recorded and depicted in Figure 4(b). The width of the upper notch (W_{n1}) varies from 4.35 mm to 9.35 mm. When the width of the antenna rises, the bandwidth of the antenna decreases, according to the return loss characteristics. As a result, it can be determined that a notch with a width of 4.35 mm provides the best bandwidth.

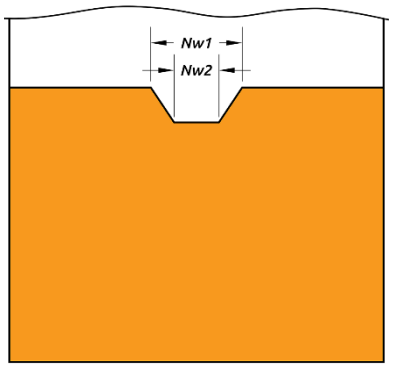

(a)

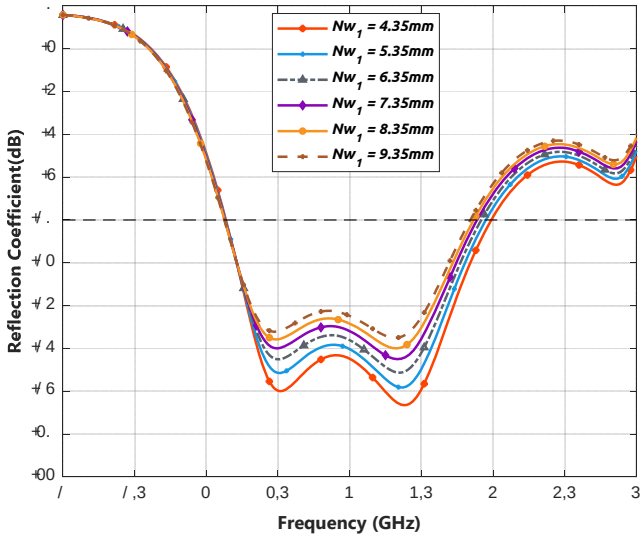

(b)

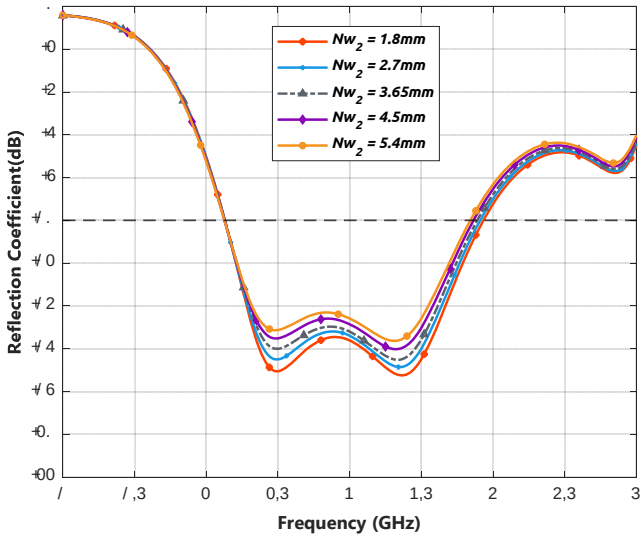

(c)

Figure 4 Parametric Analysis with Notch Width (a) Antenna, (b) Impact on Return Loss Characteristics due to upper width W_{n1} and (c) Impact on Return Loss Characteristics due to bottom W_{n2}

3.4 Impact of Parameter Notch Lower Width (W_{n2}) of Ground Notch

The notch width W_{n2} was changed to observe the effect of a smaller notch width on the antenna performance. Refer to Figure 4(a) for the top width of the notch formed on the ground plane opposite the patch and feedline joint. During variation, the return loss characteristics were recorded and depicted in Figure 4(c). The width of the bottom Notch (W_{n2}) varies from 1.8 to 5.4 mm. When the width of the antenna rises, the bandwidth of the antenna decreases, according to the return loss characteristics. As a result, it can be inferred that the notch width of 1.8 mm is the best width for obtaining a broader bandwidth.

3.5 Impact of Parameter Feedline Width (F_w)

It is modified to observe the effect of feedline width Fw on antenna performance. F_w refers to the feedline width on the patch plane (see Figure 5(a)). The features of return loss during the variation in F_w have been recorded and shown in Figure 5(b). Fw varies between 1.5 and 3 mm. When F_w is increased by 3 mm, the antenna's bandwidth shifts from lower to higher without causing any substantial changes; just the resonant frequency shifts from left to right. As a result, it can be determined that a feedline width of 2.5 mm is the best width for matching the antenna's correct impedance.

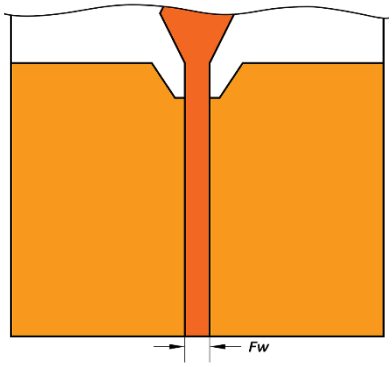

(a)

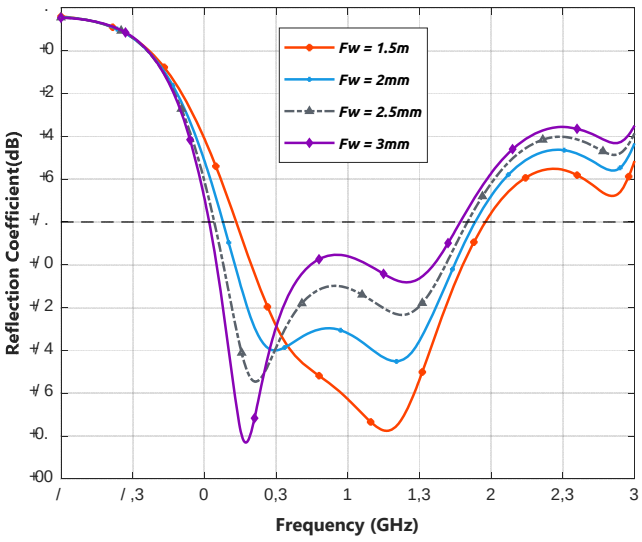

(b)

Figure 5 Parametric Analysis with Feedline Width (F_w) (a) Antenna (b) Impact on Return Loss Characteristics

3.6 Impact of Parameter Feedline Length (F_l)

It is modified to see the effect of feedline length F_l on antenna performance. Refer to Figure 6(a) for the feedline length on the patch plane. The features of return loss during variation have been recorded and are depicted in Figure 6(b). F_l ranges from 17 to 22 mm, with a 1 mm step size. The return loss characteristics show that as F_l rises, the antenna's bandwidth increases. As a result, a change in feedline length will result in a large change in antenna performance.

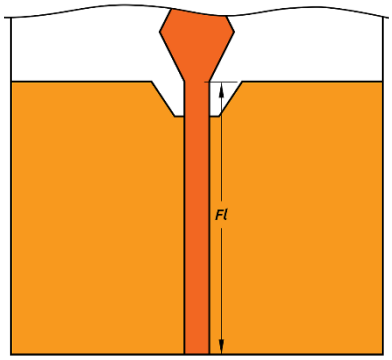

(a)

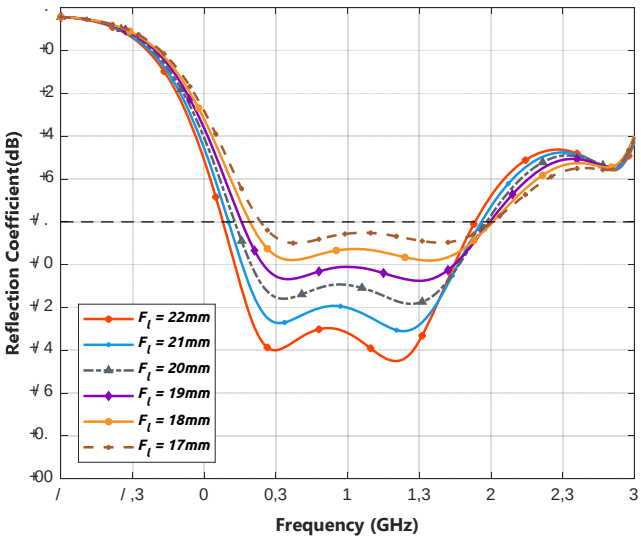

(b)

Figure 6 Parametric Analysis with Feedline Length (F_l) (a) Antenna (b) Impact on Return Loss Characteristics

IV. EXPERIMENTAL RESULTS AND DISCUSSION

4.1 Return Loss Characteristics

The optimized Antenna gives a good return loss curve at a lower cut-off frequency of 2.134 GHz and a higher cut-off frequency of 3.886 GHz, according to the return loss characteristics of the given antennas. The proposed fabricated antenna appropriate for WLAN applications, as shown in Figure 7. Return loss curve shown in Figure 8, we can see that the improved antenna resonates at 2.94 GHz and 3.334 GHz.

The designed antenna has provided the fractional bandwidth of 58.206 % from 2.134 to 3.886 GHz frequency band calculated using Equation (1).

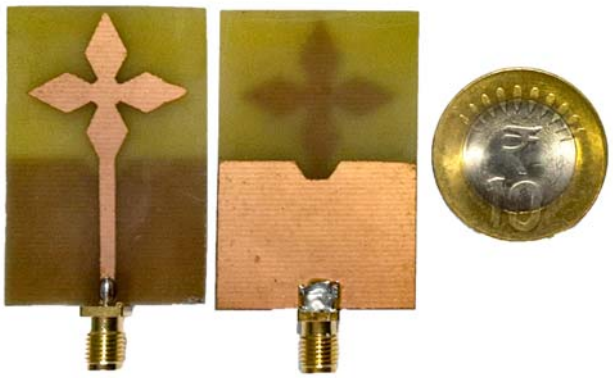

Figure 4.7 Fabricated Antenna Hardware front view (patch) and back view (ground)

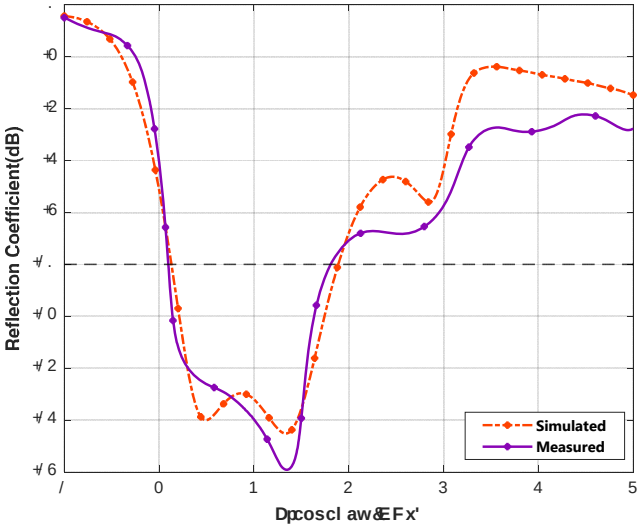

Figure 8 Reflection Coefficient of Simulation vs Measured

4.2 Surface Current Distribution

In CST, the resonant frequencies 2.494 GHz and 3.334 GHz were utilized to analyses the current distribution on the antenna surface, respectively. This study aids in determining which component of the antenna are in charge of generating a certain frequency range. Figure 9 depicts the results of the simulation run in CST-MWS.

4.2.1 First Resonance

The current vectors originate from the feedline's bottom and move towards the patch triangle's top at the first resonance frequency of 2.494 GHz. Current vector intensities are highest near the patch triangle and feedline intersection. The side borders of the patch produce a 2.494 GHz frequency signal. This path runs from the feedline's lower end to the patch triangle's top side. Equation can be used to determine the current path (2).

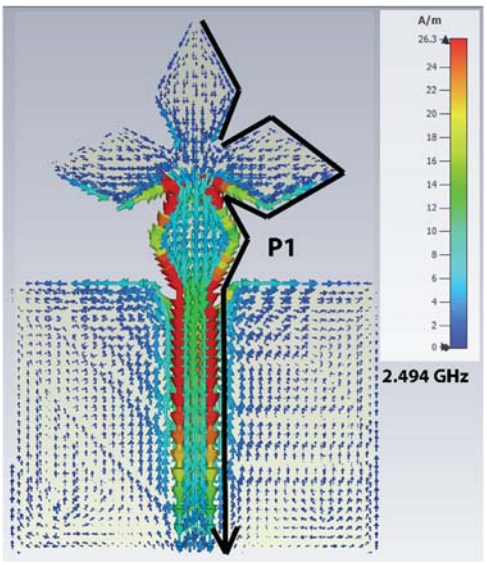

(a)

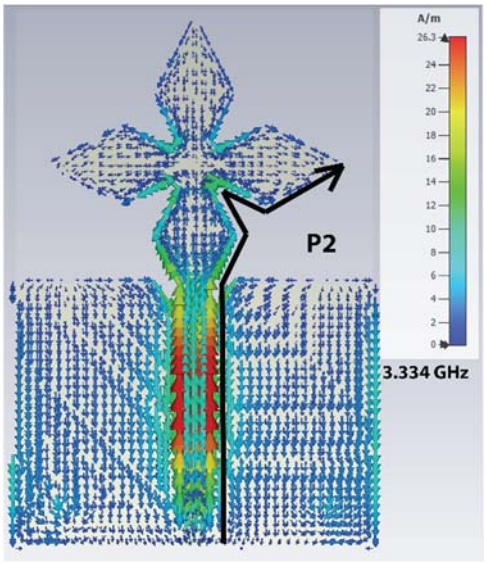

(b)

Figure 9 Surface Current Distribution on Resonant Frequencies (a) 2.494 GHz, and (b) 3.334 GHz

$$P_1 = 3\,(S_1 + S_2) + F_l + 2 \times S_3 \quad \ldots (1)$$
$$= 58.36\ mm$$

The current path P_1 has an estimated length of 58.36 mm, and the determined value of f_{r1} is 2.61 GHz (using Equation 3). The discrepancy between the calculated and real frequency is 4.65%. Environmental conditions and other losses can contribute to this.

$$f_{r1} = \frac{c}{P_1\sqrt{\varepsilon_r}} \quad \ldots (2)$$

4.2.2 Second Resonance

The current vectors in the ground plane sink at the corners at the second resonance frequency of 3.334 GHz, resulting from notch travelling through the edges. As a result of the

current research, it is obvious that 3.334 GHz frequency signals are produced by the ground plane's side edges from the notch to the bottom corner. Equations can be used to find the next path (4).

$$P_2 = 2(S_1 + S_2) + F_l + S_3 \quad \ldots (3)$$
$$= 44.77\ mm$$

The current route P_2 has a predicted length of 44.77 mm, and the resonance frequency f_{r2} has been calculated to be 3.401 GHz (using Equation 5). The difference between the calculated and real frequency is 2%. This can be caused by environmental factors as well as other losses.

$$f_{r2} = \frac{c}{P_2\sqrt{\varepsilon_r}} \quad \ldots (4)$$

4.3 Far-Field Pattern

The findings of the examination of simulated and measured far-field radiation patterns were found to differ slightly due to the surrounding environment of measuring devices or fabrication mistake (refer Figure 10). A Far-field pattern has been discovered at the resonating frequencies of 2.494 GHz and 3.334 GHz, which is omnidirectional in H-Plane and bidirectional in E-Plane. Due to dielectric loss, the efficiency of the provided antenna has decreased (see Figure 13). The suggested antenna's realized gain ranges from 0.85 to 1.06 dBi (see Figure 14).

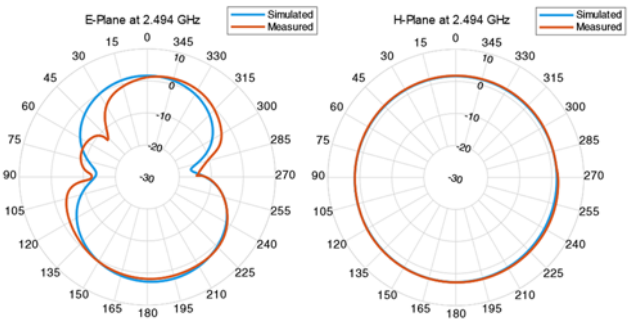

(a)

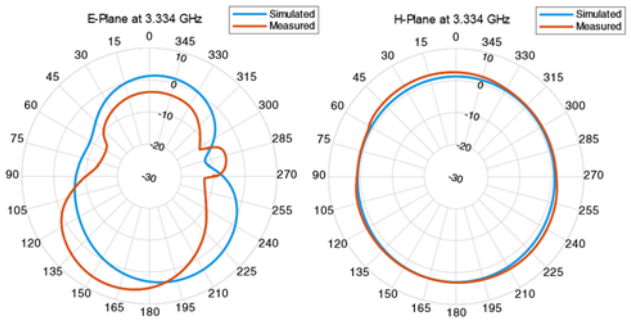

(b)

Figure 10 2D Far-field Radiation Patterns of E and H Planes at (a) 2.494 GHz, and (b) 3.334 GHz

4.4 Input Impedance

Figure 11 shows the input impedance of the planned antenna. The presence of several loops inside the VSWR circle implies mutual coupling and overlapping between resonating modes, both of which are required for a large impedance bandwidth (refer to Figure 12).

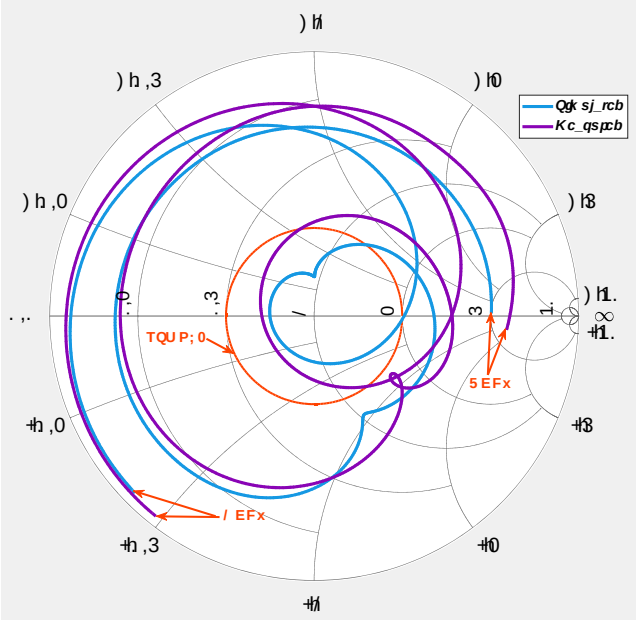

Figure 11 Impedance Curve

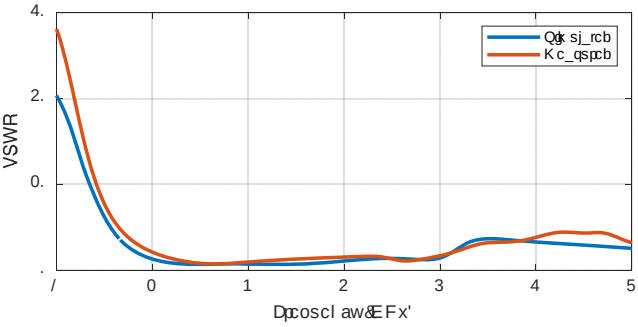

Figure 12 VSWR (Simulated) Curve of the proposed antenna

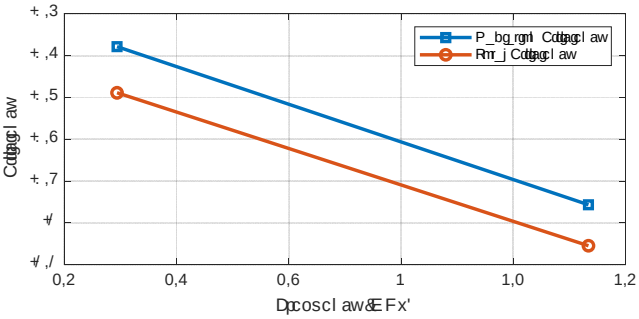

Figure 13 Simulated Radiation efficiency and Total Efficiency of the proposed antenna

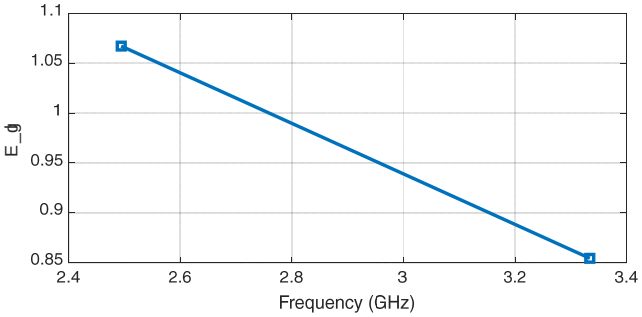

Figure 14 Gain of Antenna

V. CONCLUSION

In this section, a Quad Rhombus Pinwheel Shaped Patch Antenna (QRPPA) is constructed and its performance is investigated in order to improve impedance bandwidth and return loss (-|S_{11}|) characteristics. Over the frequency range of 2.134 GHz to 3.886 GHz, optimized QRPPA achieves a fractional bandwidth of 58.206 percent for |S_{11}| -10dB. At resonating frequencies of 2.494 GHz and 3.334 GHz, radiation patterns and current distribution were examined, and found to be omnidirectional at resonating frequencies with 1.06 dBi gain. The simulation and measurement results reveal that the proposed antenna is a good fit for wideband applications like WLAN.

REFERENCES

[1]. C. A. Balanis, Antenna Theory: Analysis and Design, 3rd ed., New York: John Wiley & Sons, 2005.
[2]. W. L. Stutzman and G. A. Thiele, Antenna Theory and Design, New York: John Wiley & Sons, 1998.
[3]. F. E. Gardiol, Introduction to Microwaves, Mass: Artech House, 1984.
[4]. D. M. Pozar, Microwave and RF Design of Wireless Systems, New York: John Wiley & Sons, 2001.
[5]. A. Q. Khan, M. Riaz and A. Bilal, "Various Types of Antenna with Respect to their Applications: A Review," International Journal Of Multidisciplinary Sciences And Engineering, vol. 7, no. 3, p. 8, March 2016.
[6]. P. M. Dickens, "Research developments in rapid prototyping," Journal of Engineering Manufacture, pp. 261-266, August 1995.
[7]. M. I. M. Ghazali, . E. Gutierrez, J. C. Myers, A. Kaur, B. Wright and P. Chahal, "Affordable 3D Printed Microwave Antennas".
[8]. R. S. Kshetrimayum, "An introduction to UWB communication systems," IEEE Potentials, vol. 28, no. 2, pp. 9-13, March-April, 2009.
[9]. S. H. Choi, J. K. Park, S. K. Kim, and J. Y. Park , "A new ultra-wideband antenna for UWB applications," Microwave and Optical Technology Letters, vol. 40, no. 5, pp. 399-401, March 5, 2004.
[10]. L. Guo, S. Wang, X. Chen, and C. G. Parini, "Study of compact antenna for UWB applications," Electronics Letters, vol. 46, no. 2, pp. 115-116, January 21, 2010.
[11]. C. Sim, W. Chung, and C. Lee, "Compact slot antenna for UWB applications," IEEE Antennas and Wireless Propagation Letters, vol. 9, pp. 63-66, 2010.
[12]. A. A. L. Neyestanak, "Ultra wideband rose leaf microstrip patch antenna," Progress In Electromagnetics Research, vol. 86, pp. 155-168, 2008.
[13]. M. N. Shakib, M. T. Islam and N. Misran, "Stacked patch antenna with folded patch feed for ultrawideband application," IET Microwave Antennas and Propagation, vol. 4, no. 10, pp. 1456-1461, 2010.
[14]. R. Zaker and A. Abdipour, "A very compact ultrawideband printed omnidirectional monopole antenna," IEEE Antenna and Wireless Propagation Letters, vol. 9, pp. 471-473, June 2010.
[15]. Q. Wu, R. Jin, J. Geng, and M. Ding, "Printed omni-directional UWB monopole antenna with very compact size," IEEE Transactions on Antennas and Propagation, vol. 56, no. 3, pp. 896–899, Mar. 2008.
[16]. J. Jung, W. Choi, and J. Choi, "A small wideband microstrip-fed monopole antenna,"IEEE Microwave Wireless Components Letters, vol. 15, no. 10, pp. 703–705, Oct. 2005.
[17]. R. Azim, M.T. Islam, and N. Misran, "Compact tapered-shape slot antenna for UWB applications," IEEE Antennas Wireless Propagation Letters, vol. 10, pp. 1190–1193, 2011.
[18]. N. Chahat, M. Zhadobov, R. Sauleau, and K. Ito, "A compact UWB antenna for on-body applications," IEEE Transactions on Antennas and Propagation, vol. 59, no. 4, pp. 1123–1131, April 2011.
[19]. S. A. Hosseini, Z. Atlasbaf, and K. Forooraghi, "A compact ultra-wide band (UWB) planar antenna using glass as substrate," Journal of Electromagnetic Waves and Applications, vol. 22, no. 1, pp. 47 59, Jan. 2008.
[20]. G. A. Deschamps, "Microstrip microwave antennas," Proc. 3rd USAF Symposium on Antennas, 1953.
[21]. R. E. Munson, "Conformal microstrip antennas and microstrip phased arrays," IEEE Transactions on Antennas and Propagation, vol. AP-22, pp. 74-78, 1974.
[22]. J. Q. Howell, "Microstrip antennas," IEEE Transactions on Antennas and Propagation, vol. AP-23, pp. 90-93, January 1975.
[23]. R. Garg, P. Bhartia, I. Bahl, A. Ittipiboon, Microstrip Antenna Design Handbook, Artech House, Norwood, MA, 2001.
[24]. [24] T.C. Edwards and M.B. Steer, "Foundations of interconnect and microstrip design", New York: John Wiley, pp. 51-64, 2000.
[25]. Y. Huang and K. Boyle, "Antennas: from theory to practice", John Wiley & Sons, 2008.